Defect Pinning in Monolayer Films by Highly Controlled Graphite Defects: Molecule Corrals

ARTICLE *in* LANGMUIR · APRIL 1996

Impact Factor: 4.46 · DOI: 10.1021/la950354h

4 AUTHORS, INCLUDING:

David L Patrick
Western Washington University
38 PUBLICATIONS **880** CITATIONS
SEE PROFILE

Timothy J. Purcell
NVIDIA
12 PUBLICATIONS **2,240** CITATIONS
SEE PROFILE

Thomas Beebe
University of Delaware
99 PUBLICATIONS **4,069** CITATIONS
SEE PROFILE

Defect Pinning in Monolayer Films by Highly Controlled Graphite Defects: Molecule Corrals

David L. Patrick, Victor J. Cee, Timothy J. Purcell, and Thomas P. Beebe, Jr.*

Department of Chemistry, The University of Utah, Salt Lake City, Utah 84112

Received May 8, 1995. In Final Form: August 7, 1995[⊗]

Domain boundaries in a self-assembled molecular film are immobilized or "pinned" for study with scanning tunneling microscopy using monolayer deep etch pits in the basal plane of graphite ("molecule corrals"). Molecule corrals are shown to provide a highly controllable method of generating substrate defects to study pinning in monolayer films. Diffusion of pinned boundaries is found to take place *via* discreet motions involving small groups of molecules. A model for grain boundary motion is developed and used to analyze two types of boundaries: those separating molecular domains with identical structures and those separating domains with different structures. When the structures are different, a "one-dimensional pressure" is exerted on the boundary by the structure with the lower free energy, causing it to distort. By measuring the dependence of this distortion on the distance between pinning centers, we extract quantitative information about certain energetic properties of the film.

Introduction

The characteristics and behavior of defects in monolayer films have been subjects of interest nearly since thin films were discovered.[1] Thin film defects, which range in type from vacancies and dislocations to orientational grain boundaries and impurities, play critical roles in determining most film properties. A number of important film characteristics, including permeability, conductivity, mechanical and chemical properties, and roughening and melting mechanisms are all thought to be dominated by defects.[2]

The importance of defects on the properties of monolayer films has made them interesting objects in their own right, and aspects of defect creation, diffusion, mutual interaction, and destruction have been widely studied.[3] Among the most technologically relevant of systems to study in this regard are commensurate molecular films on solid substrates, since they include self-assembled monolayers, a new and very promising class of molecular thin films. An interesting aspect of defects in commensurate monolayer films involves their interaction with defects in the underlying substrate. Below a certain critical temperature, film defects can be attracted to, and fixed in place ("pinned") by substrate defects. Although defect pinning is an important phenomenon, it has traditionally been difficult to study, since in general it is impossible to control with accuracy the nature of substrate defects at length scales relevant to pinning of defects in monolayer films.

This work describes a solution to the problem of substrate defect control by using "molecule corrals" as highly controllable surface defects. Molecule corrals are nanometer-sized circular pits formed on the basal plane of pyrolytic graphite by high temperature oxidation. Although molecule corrals have previously been used to contain and study small numbers of molecules in their interiors,[4] their highly controllable size, shape, and surface density also make them ideal for use as model substrate defects. By combining corrals (albeit in a noncorralling role) with scanning tunneling microscopy (STM), it is possible to probe details of the pinning mechanism, as well as the energetics and dynamics of grain boundary motion at molecular length scales.

Experimental Section

Samples used in this study were prepared by depositing a small drop of the liquid crystal 4′-octyl-4-cyanobiphenyl (8CB) onto oxidized graphite. 8CB self-assembles on graphite to form large monolayer domains of nearly perfect crystallinity.[5] Domains consist of rows of molecules aligned in a head-to-head configuration, similar to the way molecules pack in a molecular bilayer. Each oblique unit cell contains eight molecules lying with thier long molecular axes in the plane of the surface.[5] Ordinarily these films contain very few defects.[6] To increase the number of grain boundaries, we therefore cooled the graphite crystals to approximately 268 K prior to application of the 8CB. Grain boundaries are one-dimensional defects caused by the in-plane intersection of misoriented crystallites. Cooling the graphite/8CB system increases the nucleation rate relative to the growth rate, resulting in the formation of additional grain boundaries. After application of 8CB, samples were warmed to room temperature and imaged with STM. Prior to the application of molecules, molecule corrals were produced by heating freshly cleaved graphite in air to 950 K for ∼15 min.[7] Several samples with differing corral sizes and densities were used, each giving similar results.

Results and Discussion

1. Diffusion of Pinned Grain Boundaries. Under the conditions used in this investigation, grain boundaries exhibit diffusional motion over time scales discernible by STM.[8] The extent of diffusion is observed to depend strongly on certain (as yet unidentified) microscopic characterstics of the STM tip. Two types of tip-related conditions exist. The first of these is one in which the grain boundary is severely perturbed by the scanning motion of the tip. When this condition occurs, a grain boundary may shift back and forth by hundreds of angstroms, its position oscillating in phase with the scanning motion of the tip. An example of this is shown

* To whom correspondence should be addressed.

[⊗] Abstract published in *Advance ACS Abstracts,* March 1, 1996.

(1) Langmuir, I. *Trans. Faraday Soc.* **1920**, *15*, 62.

(2) Ulman, A. *An Introduction to Ultrathin Organic Films From Langmuir-Blodgett to Self-Assembly*; Academic Press: New York, New York, 1991.

(3) Lyuksyutov, I.; Naumovets, A. G.; Pokrovsky, V. *Two-Dimensional Crystals*; Academic Press: New York, New York 1992.

(4) Patrick, D. L.; Cee, V. J.; Beebe, T. P. Jr. *Science* **1994**, *265*, 231.

(5) Foster, J. S.; Frommer, J. E. *Nature* **1988**, *333*, 542.

(6) Smith, D. P. E. J. *Vac. Sci. Technol., B* **1991**, *9*, 1119.

(7) Chang, H.; Bard, A. J. *J. Am. Chem. Soc.* **1990**, *112*, 4598. Chu, X.; Schmidt, L. D. *Carbon* **1991**, *29*, 1251.

(8) For examples of diffusional behavior in other organic systems studied by STM see: Parks, D. C.; Clark, N. A.; Walba, D. M.; Beale, P. D. *Phys. Rev. Lett.* **1993**, *70*, 607. Ludwig, Ch.; Eberle, G.; Gompf, B.; Peterson, J.; Eisenmenger, W. *Ann. Phys.* **1993** *2*, 323. Rabe, J. P.; Buchholz, S. *Phys. Rev. Lett.* **1991**, *66*, 2096.

0743-7463/96/2412-1830$12.00/0

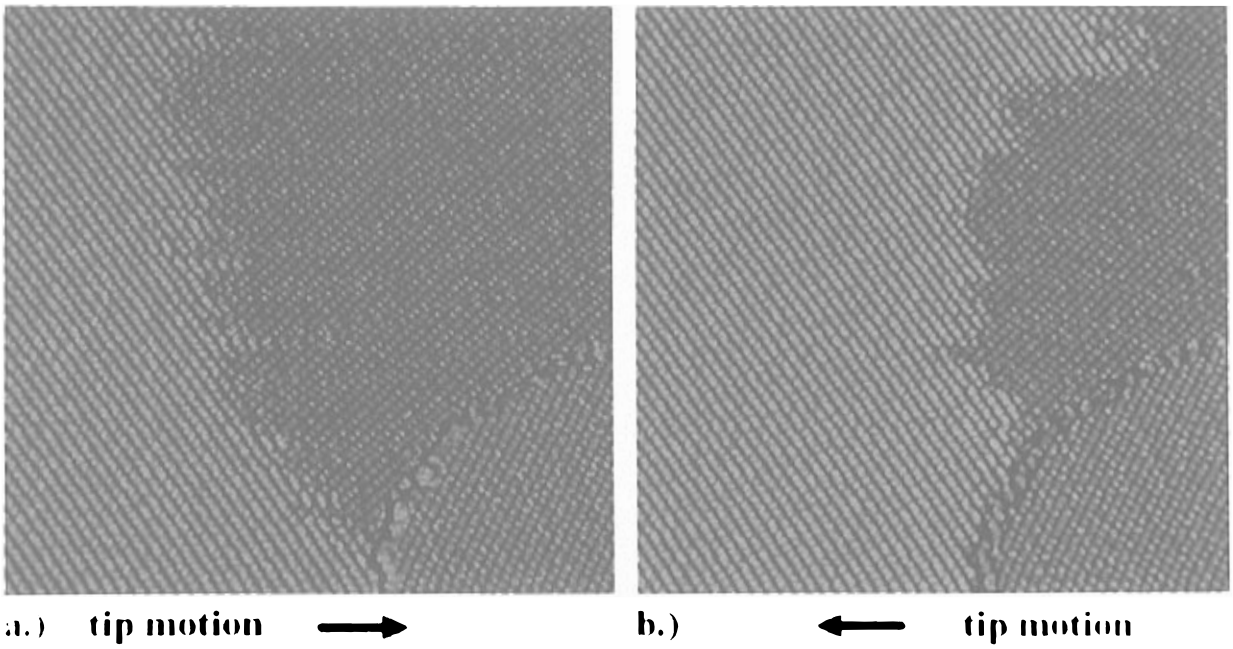

Figure 1. Two complementary images of a pinned domain boundary taken with a highly perturbing tip: (a) data acquired as the STM tip scanned from left to right; (b) data acquired as the tip scanned from right to left. The corral in the lower right corner serves as a reference to indicate the large difference in the position of the boundary in the two images. Images measure 2600 Å × 2600 Å, $V_{bias} = -0.69$ V, $I_{tunn} = 90$ pA, scan speed = 6.64 μm s^{-1}.

in Figure 1, which presents two complementary images demonstating the effect of a strongly perturbing tip. The first image (part a) is composed of pixels collected as the tip was scanned from left to right, while the image in part b was formed from pixels collected as the tip scanned from right to left. Although both images are of the same region (as indicated by the corral in the lower right corner), and both images were collected at the same time (with alternating lines collected sequentially), the position of the domain boundary in the two images is markedly different, shifting by over 1000 Å in some places.

The second type of tip-related imaging condition, in stark contrast to the first, occurs when the tip exerts no detectable influence on grain boundaries. When a tip is relatively nonperturbing, complementary images such as those in Figure 1 are virtually indistinguishable. Frequently a tip can be interconverted between these two types (perturbing vs nonperturbing) by application of a short, ~5 V pulse to the bias voltage. Voltage pulses of this kind are believed to alter the microscopic structure of the end of the tip,[9] suggesting that tip−grain boundary interactions may occur through mechanical or electrical means. In this study we only report data collected with the second, relatively nonperturbing tip type (with the exception of Figure 1).

Using a relatively nonperturbing tip, diffusional motion of grain boundaries is still observed. Two types of motion are most prevalent, occurring on two very different time scales. The more rapid of these motions is associated with small groups of molecules interchanging between the two domains, a process giving rise to what has been called "frizziness" in the STM image at the boundary. Frizziness in an STM image is caused by motion of the specimen object occurring on a time scale less than or equal to the rate of data acquisition.[10] An effective way of capturing data about this type of motion with STM is to collect a "time image". A time image is formed by repeatedly scanning the same line in the *x* dimension while not moving in the *y* dimension, *i.e.*, by imaging a region of zero length but nonzero width. The "image" formed has a spatial dimension along the *x*-axis and a time dimension along the *y*-axis. This approach offers the advantage of combining high spatial resolution (in one dimension only) with increased temporal resolution and is useful for studying diffusional motion too rapid to easily discern in a traditional imaging mode.

Figure 2a shows a time image formed by repeatedly scanning the tip accross the grain boundary at the horizontal line marked in the conventional image shown in Figure 2b. Each of the 512 lines in Figure 2a was acquired 50 ms apart at a rate of 4.9×10^{-5} s pixel^{-1}. The average position of the boundary is marked by the frizzy band near the center of the image. Approximately two-thirds of the the way through acquisition of the image, the average position of the boundary shifted (indicated by the arrow). This was followed ~15 s later by the return of the boundary to its previous position (not shown).

Inspection of this figure reveals grain boundary motion occurring on several different time scales. The most rapid motion detectable is a high frequency oscillation of the grain boundary about its mean position.[11] It is this oscillation that gives rise to frizziness in the image. Since the position of the boundary is rarely the same for two scan lines in a row, the frequency of the oscillation is at least 20 Hz, and probably much greater. The amplitude of the oscillation is approximately ± 75 Å about the mean.

The second type of motion, which occurs less rapidly, is an occasional shift in the average position of the grain boundary. These shifts, one of which is shown in Figure 2a marked by an arrow, occur every 10−30 s. Over time they appear to cancel one another, leading to no net motion of the boundary. Interestingly, these shifts occur in discreet jumps rather than through a continuous motion. This is demonstrated in Figure 2c, which compares cross sectional data taken from Figure 2a during the time

(9) Chen, C. J. *Introduction to Scanning Tunneling Microscopy*; Oxford University Press: Oxford, 1993.

(10) Giesen-Seibert, M.; Jentjens, R.; Poensgen, M.; Ibach, H. *Phys. Rev. Lett.* **1993**, *71*, 3521. Kuipers, L.; Hoogeman, M. S.; Frenken, J. W. M. *Phys. Rev. Lett.* **1993**, *71*, 3517. Dunphy, J. C.; Sautet, P.; Ogletree, D. F.; Salmeron, M. B. *J. Vac. Sci. Technol., A* **1993**, *11*, 2145.

(11) The mean is defined as the average position of the grain boundary during the last few seconds.

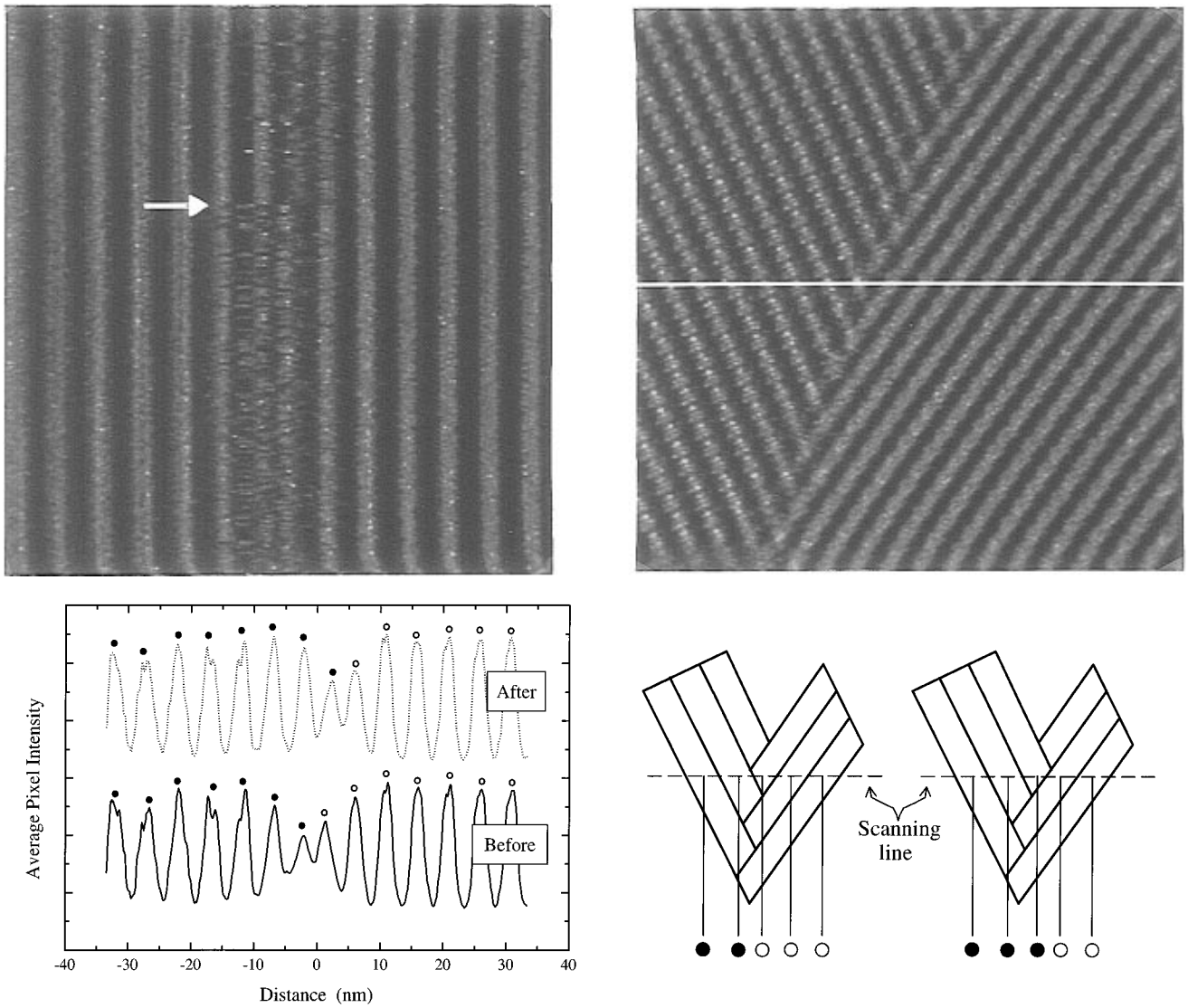

Figure 2. (a, top left) An STM "time image" formed by repeatedly imaging the highlighted scan line in the conventional image in part b ($V_{bias} = -0.41$ V, $I_{tunn} = 86$ pA). The image was acquired in constant height mode and measures 650 Å horizontally × 25.6 s vertically. The narrow vertical band of distortion was caused by rapid motion of the boundary. A change in the average position of the boundary is marked by the arrow. (b, top right) 850 Å x 850 Å constant height image of a grain boundary ($V_{bias} = -0.36$ V, $I_{tunn} = 90$ pA, scan speed = 3.92 μm s^{-1}). The image is a pixelwise average of five consecutive images, individually corrected for thermal drift using a least-squares minimization criterion.[12] (c, bottom left) The solid and dotted curves are, respectively, averages of line scans from the time image taken before and after the change in the boundary's average position marked by the arrow in part a. Solid and open circles identify each peak in the scan line with the location of a molecular row from the left or right domain as shown in part d. Note that the position of the boundary has shifted to the right by an amount equal to the spacing between the solid circles. (d, bottom right) Conceptual model illustrating the origin of discreet changes in grain boundary positions like that shown in part c. Molecular rows to the left of the boundary produce rows in the time image centered on the solid circles while those to the right of the boundary produce rows centered on the open circles. A single-row shift in the position of the boundary causes the pattern of rows in the time image to shift by a proportionate amount.

intervals preceding and following the shift. The data are line-by-line averages over each interval (all scan lines preceding the shift were averaged together to give the solid curve and all scan lines following the shift were averaged together to give the dotted curve). Comparison of the two curves shows that the position of the boundary has shifted by ~50 Å along the horizontal.

Notice that the envelope of the oscillation profile in Figure 2c decays to approximately the average of the extremes at the boundary. To understand the origin of the two smaller peaks occurring at this position in terms of a change in the location of the boundary, we make use of the fact that the period of the oscillation is slightly different in the two domains (49.1 ± 1 and 50.8 ± 1 Å for the left and right domains, respectively). This difference arises from slight differences in the inter-row molecular spacings of the two domains, as well as from the relative orientation of rows in the two domains with respect to the tip scan direction (the horizontal direction). By measuring the spacing between adjacent peaks, it is therefore possible to assign each of them as belonging to either the left or the right domain. Using this approach, peaks from the left domain are labeled with solid circles and those from the right domain are labeled with open circles. With peaks labeled in this way it becomes clear that the shift was produced when a group of molecules at the boundary initially belonging to the domain on the right rearranged to align with those in the domain on the left. Figure 2d shows schematically how the extension of a molecular row from the left domain into the right domain could produce the shift observed in Figure 2c.

Additional evidence for the existence of these position shifts is shown in Figure 2b. This image is a pixelwise average of five consecutive images, individually corrected

for thermal drift.[12] Inspection of the boundary shows that at certain locations it does not seem to have a well-defined position. In these sections the molecular rows have a cross-hatched appearance, as if overlapping one another. This effect is caused by jumps in the position of the boundary between collection of the individual images making up the composite time-average in Figure 2b. When images showing sections of the boundary that have shifted are averaged together, molecular rows of the two domains appear superimposed, giving the impression they overlap. In fact it is clear from Figure 2a, having higher temporal resolution, that only one row is present at a time and no actual overlap occurs.

2. Energetics of Grain Boundary Distortion. Inspection of Figure 2b reveals that the molecular rows on either side the grain boundary are spaced slightly differently (45.6 ± 1 Å vs 40.0 ± 1 Å) and that they form an intersection angle of 62°. This difference in spacing means that the molecules are organized slightly differently in the two domains.[13] As a result, the two configurations can be expected to possess slightly different Gibb's free energies. A free energy difference between domains can produce a net diffusive motion of grain boundaries, since through motion of the domain boundary the molecular structure of lower free energy can gradually replace the one of higher free energy and the overall energy of the system will be reduced. It is in this way, through the diffusion of domain boundaries, that the system approaches an equilibrium distribution of phases.

On a defect-free substrate, the diffusion rate of grain boundaries is limited only by the rate of formation of kink−antikink pairs.[14] However when substrate defects are present, they may create additional barriers toward diffusion. These barriers, if large compared to the available thermal energy, can inhibit grain boundary motion through a process known as pinning.

An example of grain boundary pinning by substrate defects is shown in Figure 3. The first part of this figure, Figure 3a, shows a boundary between molecular domains pinned by several corrals. The image has been displayed with a derivative-based color scale (i.e., "shaded") to enhance the contrast of the two domains. Figure 3b shows a large-scale view of the paths taken by several grain boundaries as they meander their way across the surface. Because they are not easily visible at the pixel density of this image, the boundaries were mapped from inspection of several higher resolution images and outlined in white.

As stated above, if a grain boundary separates two distinct phases, the overall free energy of the system may be lowered by the gradual replacement of the higher energy phase with the lower energy one. If the boundary is pinned, however, its diffusive motion may be greatly impeded by kinetic and/or thermodynamic barriers. In this case, motion of the boundary resulting in the replacement of the higher energy phase by the lower energy phase is counterbalanced by the line energy of the boundary. A clear example illustrating the result of these competing effects is shown in Figure 4a and on the cover. The grain boundary has shifted position away from the shortest path between pinning centers, increasing the area occupied by the phase in the lower half of the image at the expense of the phase in the upper half of the image. These findings suggest that it should be possible to learn something about the relative values of the energy between phases and the line energy of their boundaries by measuring the amount of boundary distortion or "bulge" from the shortest path between defects. To investigate this further, we developed a model in which the free energy is a function of just four variables (refer to Figure 4b). For simplicity, we model the bulge as a circular section and assume that the line energy is the same everywhere along its length. These assumptions are valid so long as the bulge remains reasonably small.

According to the parameters defined in Figure 4b, the amount of bulge b resulting in a minimization of the free

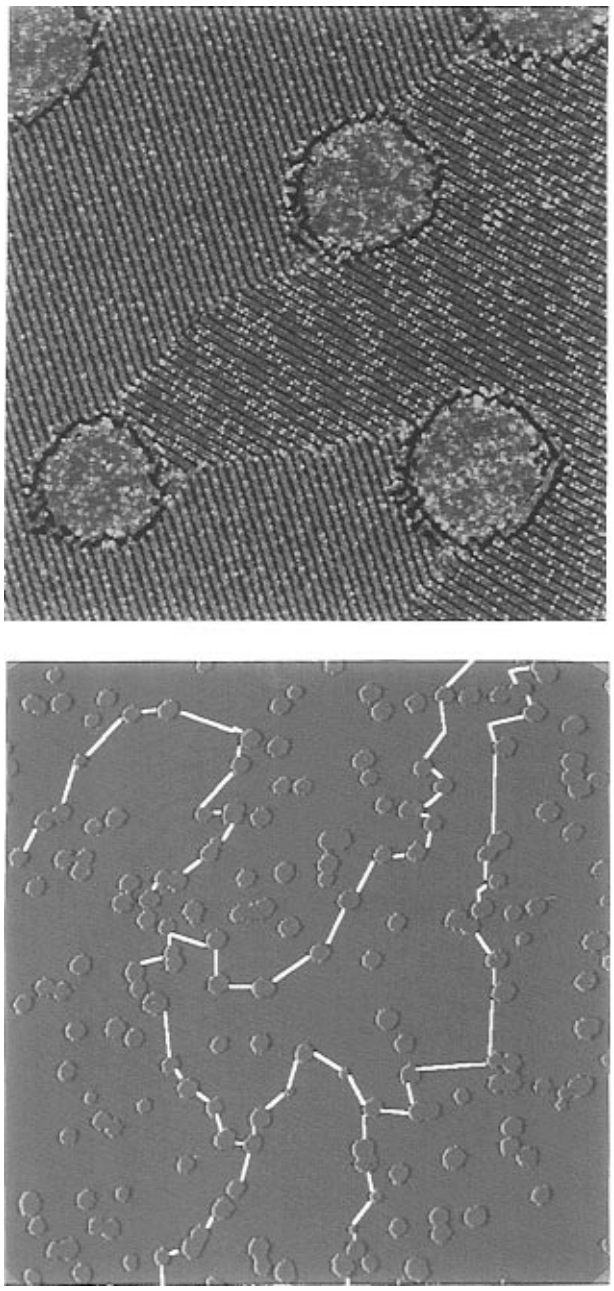

Figure 3. (a, top) 3200 Å × 3200 Å constant height image of ordered 8CB molecules on graphite ($V_{bias} = -0.89$ V, $I_{tunn} = 100$ pA, scan speed = 7.89 μm s^{-1}). The circular features are molecule corrals produced prior to the application of molecules and are used as highly controlled defects to pin diffusing grain boundaries in the self-assembled molecular film. Note how the boundary follows nearly the shortest path between corrals. The image is shown with a derivative-based color scale to enhance the contrast of the two domains. (b, bottom) A 2 μm × 2 μm constant height image of an area containing multiple domains ($V_{bias} = -0.89$ V, $I_{tunn} = 96$ pA, scan speed = 12.21 μm s^{-1}). The boundaries have been marked in white. At the scale of this image, and given the pixel density, molecular rows are no longer discernible.

(12) Patrick, D. L.; Beebe, T. P., Jr. Submitted for publication in *Anal. Chem*.
(13) Patrick, D. L.; Beebe, T. P., Jr. *Langmuir* **1994**, *10*, 298.
(14) Hirth, J. P.; Lothe, J. *Theory of Dislocations*; McGraw-Hill: New York, 1967.

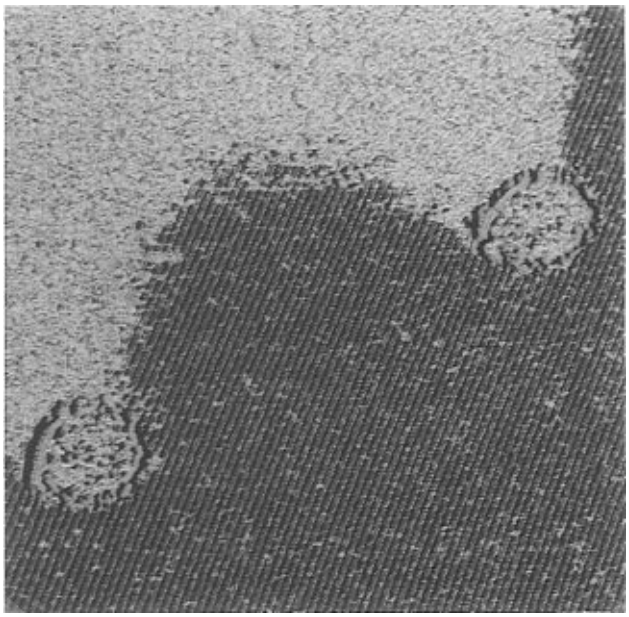

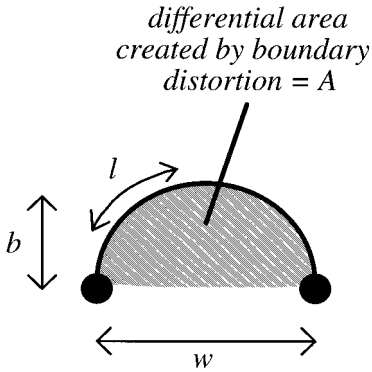

Figure 4. (a, top) 3500 Å × 3500 Å STM image showing a pinned grain boundary with an unusally large amount of distortion ($V_{bias} = -0.95$ V, $I_{tunn} = 85$ pA, scan speed = 9.92 μm s^{-1}). Note the nearly circular shape of the boundary. Image is shown with a derivative-based color scale to enhance the difference between the two domains, making the molecular rows in the upper half of the image difficult to discern. This boundary represents an extreme case in which the amount of distortion is comparable to the distance between pinning centers. Because of this, it was very unstable and frequently shifted from one set of pinning centers to another. (b, bottom) Definition of quantities used to model the amount of grain boundary distortion (refer to text).

energy is determined by the distance w between pinning defects, the line energy σ of the domain boundary, and the free energy difference per unit area between the two domains E_A. The lower energy phase can occupy an additional area $A = (1/2)[lr - w(r - b)]$ by distorting the grain boundary from its shortest path w by an amount b. The quantity $r = (w^2/8b) + (b/2)$ is the radius of curvature of the region created by the bulge, and $l = 4r \arctan(2b/w)$ is its arc length. The free energy change resulting from the bulge is then $\Delta E = AE_A + l\sigma - E_0$, where $E_0 = w\sigma$ is the energy of the boundary in the absence of any bulge.

Figure 5 shows ΔE plotted against b for two values of hypothetical σ/E_A. Because the area of the region produced by the bulge scales as b^2 while the perimeter scales as b, a pinned grain boundary is at best metastable, and in some cases unstable toward distortion. The two cases are illustrated in Figure 5 by solid and dotted curves, which represent metastable and unstable conditions, respectively. Whether or not a pinned domain is metastable depends on the ratio σ/E_A as well as the distance between pinning centers w. In general, a pinned domain

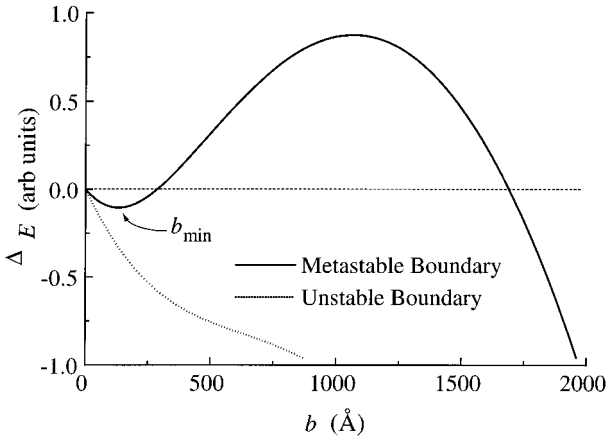

Figure 5. A pinned grain boundary can be either unstable or metastable, depending on the line tension of the boundary, the free energy difference of molecules in the two domains, and the distance between pinning centers. Metastable boundaries undergo a small distortion from linearity by moving to the local free energy minimum at b_{min}, whereas unstable grain boundaries spontaneously distort without limit. See Figure 4b for a definition of b_{min}.

will be unstable toward distortion if $|\sigma/E_A| < w/2$, and metastable if $|\sigma/E_A| > w/2$. Thus according to the model used here, only substrate defects that are relatively close together are able to pin a grain boundary in a metastable condition.

If a pinned boundary is unstable, it will distort spontaneously, migrating until the lower energy phase entirely consumes the higher energy one. However a metastable boundary will initially distort only slightly, just enough to reach the local minimum shown in Figure 5. The position of this minimum can be calculated[15] by setting $\partial\Delta E/\partial b$ equal to zero and solving for b:

$$b_{min} = \pm\frac{w}{4}\left(\frac{2\sigma}{wE_A} - 1\right)^{-1/2} \qquad (1)$$

A pinned grain boundary will thus remain fixed with an average bulge b_{min} until thermal fluctuations impart it sufficient energy to break free.

Using eq 1 it is possible to estimate the ratio σ/E_A from measurements of the dependence of the average bulge b on w. Figure 6 illustrates this dependence for two domain boundaries. Each data point represents a measurement of the amount of bulge b of a domain boundary segment pinned by corrals separated by a distance w, where b and w can be accurately measured from STM images. The open circles plotted in Figure 6 are from a grain boundary separating two domains in which the molecular rows had slightly *different* spacings (44.3 ± 1 Å *vs* 40.6 ± 1 Å, intersection angle 36 ± 3°). As discussed above, different row spacings are expected to correspond with different configurational free energies in the two domains: the boundary's energetics dominates the distortion behavior and resulting domain size. The expectation is confirmed by the data, which show an overall increase in the bulge b with defect separation length w. A fit of equation 1 to the open circles (solid line) gives a ratio $\sigma/E_A = (1.38 \pm 0.08) \times 10^5$ Å. In normalized units the line energy of the boundary is thus much larger than the free energy difference of the two domains. The grain boundary from

(15) To find an expression for location of the local minimum, we use a simplifying approximation for ΔE, valid at small amounts of distortion when $b \ll w$

$$\Delta E_{b \ll w} = \frac{1}{2} wbE_A + 2\sigma\left(b^2 + \frac{w^2}{4}\right)^{1/2}$$

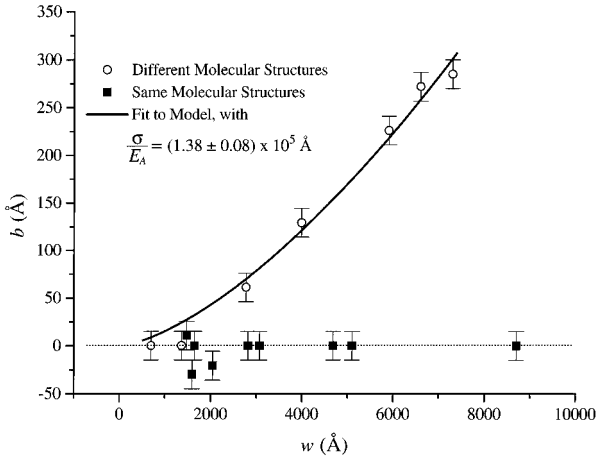

Figure 6. Open circles show the distortion b of a grain boundary separating two domains of *unequal* free energy *vs* the distance between pinning centers w. The solid line is a least-squares fit of equation 1 to the data with $\sigma/E_A = (1.38 \pm 0.08) \times 10^5$ Å (refer to text). Solid squares represent the average distortion of a grain boundary separating two domains of *equal* free energy. Note the lack of any systematic relationship between b and w.

which these measurements were taken was observed to occasionally depin and move from one set of pits to another. Between these motions, which may be caused by thermal fluctuations and which are too rapid to measure with our instrument, the boundary would spend relatively long periods of time (∼minutes) pinned. This type of behavior is consistent with a metastable grain boundary, as expected from the metastability condition derived above, and given that the average spacing between pinning centers w is ∼5000 Å (*i.e.* $\sigma/E_A = 1.38 \times 10^5$ Å $\gg w/2 =$ 5000/2 Å).

Figure 6 also shows a second set of data (filled squares), which were taken from measurements of the bulge of a grain boundary separating two domains in which the molecular rows had *identical* spacings but different orientations (50 ± 1 Å, intersection angle 136°). In this case, the two domains should have identical configurational free energies ($E_A = 0$). The expectation, confirmed by the plot (solid squares), is of no overall correlation between b and pinning distance w since any distortion of the boundary away from the shortest path between pinning centers will only increase the energy. Grain boundary segments as long as 8700 Å in length showed no measurable bulge. Thus the model, although simple, quantitatively accounts for the observed differences in grain boundary distortion for the cases when the two domains have different as well as equal free energies.

The model for grain boundary distortion developed here is based entirely on thermodynamic arguments. It is of interest however to consider a very different interpretation based on *mechanical* considerations. Adopting this viewpoint, distortions can be thought of as arising from a "one-dimensional pressure" exerted on the boundary by the free energy difference between the two domains. Similarly, the line energy of the domain can be considered as a line tension. These two quantities are analogous to surface pressure and surface tension in a three-dimensional system. Thought of in this way, a grain boundary will distort until the force arising from this one-dimensional pressure is exactly balanced by the force arising from the line tension.

Conclusion

We have used molecule corrals as highly controllable substrate defects to study domain boundary pinning in monolayer films and developed a model that explains in quantitative form the trends observed. Boundaries will be pinned in metastable configurations by substrate defects so long as the ratio of the line energy to the free energy difference is greater than half the distance between pinning centers. Two types of distortion in grain boundaries are described. The first arises from thermal fluctuations and/or tip-induced perturbations in the local position, which are rapid on the time scale of the STM experiment, and produce frizziness in the images. The second type of grain boundary distortion operates over longer time periods, and arises from free energy differences between molecules in adjacent domains. The observation that domain boundaries are in general only slightly distorted is in accordance with a calculation here that the line energy, rather than the free energy difference of molecules in the two domains, is the most important energetic factor in determining the properties of pinned boundaries in this system.

Acknowledgment. This work was supported by the National Science Foundation (NSF-NY1 CHE-9357188) and the Camille & Henry Dreyfus Foundation.

LA950354H